

# Molecular and Functional Properties of Acid-Sensing Ion Channels

Subjects: Physiology

Contributor: Clément Verkest, Miguel Salinas, Sylvie Diochot, Emmanuel Deval, Eric Lingueglia, Anne Baron

Acid-sensing ion channels (ASICs) are voltage-independent H<sup>+</sup>-gated cation channels largely expressed in the nervous system of rodents and humans, and involved in pain sensing and associated pathologies. At least six isoforms (ASIC1a, 1b, 2a, 2b, 3 and 4) associate into homotrimers or heterotrimers to form functional channels with highly pH-dependent gating properties.

Keywords: ASIC ; sodium channels ; toxins ; peptide ; PcTx1 ; APETx2 ; MitTx

---

## **1. Subunits Diversity and Structure**

Functional acid-sensing ion channels (ASICs) are formed by the homo- or heterotrimeric association of identical or homologous subunits <sup>[1][2][3]</sup> (**Figure 1A**), each subunit comprising more than 500 amino acids and two transmembrane domains, a large extracellular loop, and intracellular N- and C-termini with a re-entrant N-terminus loop (**Figure 1B,C**).

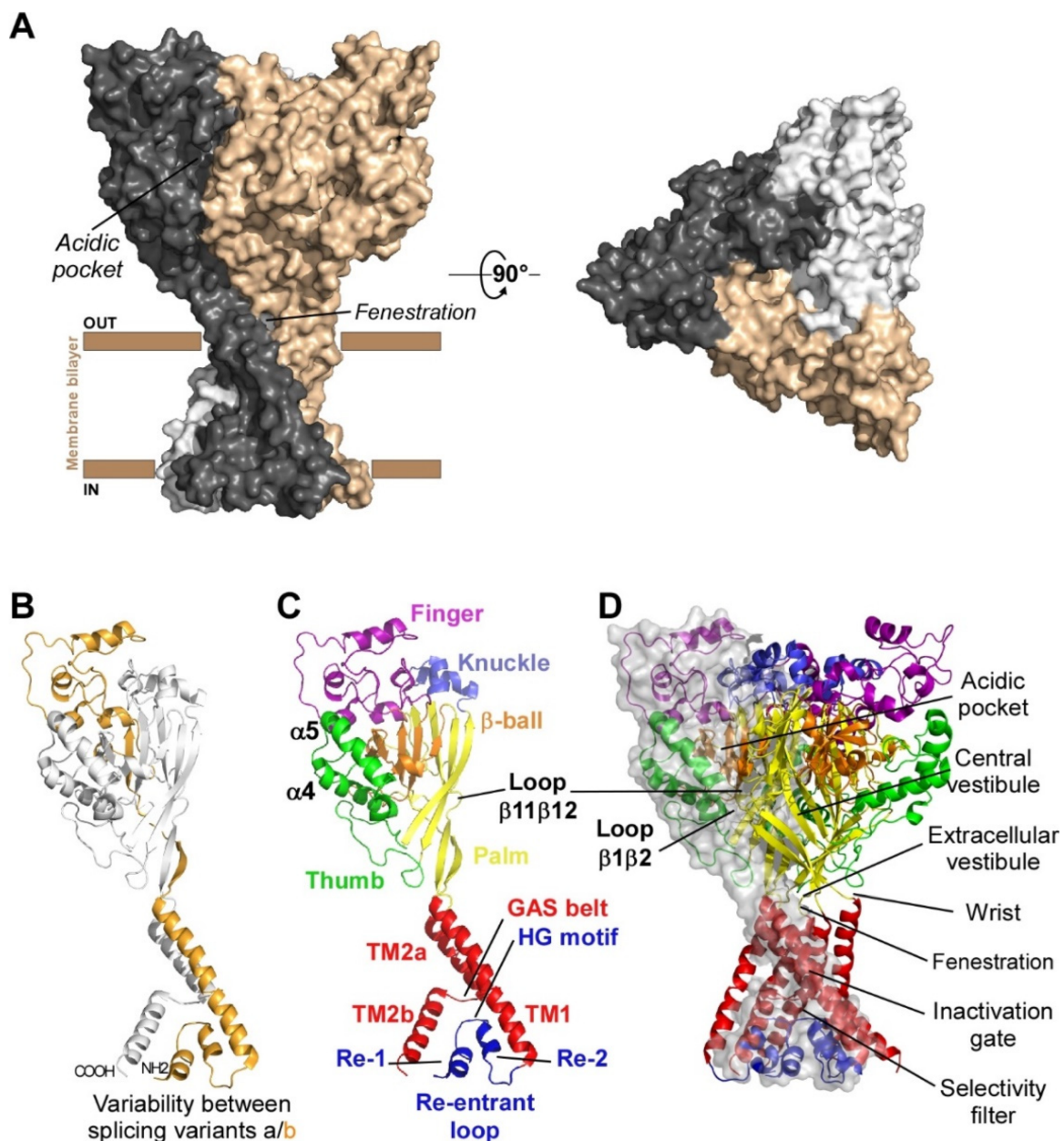


**Figure 1. Structure of ASICs.** (A) Trimeric organization of ASICs (left panel: side view, right panel: top view). (B) Tridimensional skeletal model of a single subunit where variable regions between isoforms “a” and “b” of rat ASIC1 and ASIC2 are highlighted in gold. (C) Structure of a single subunit of chicken ASIC1 in resting state (the different sub-domains are shown in specific colors; PDB ID: 6vtl). (D) Skeletal 3D representation of a functional channel formed by the assembly of three subunits. A transparent grey surface was added to one subunit to delineate the interface between two adjacent subunits. Same colors as in (C) for the different sub-domains, and key structural domains mentioned on the right. Cytoplasmic N- and C-termini, whose structures are unknown, are not shown. Designed with PyMOL software.

Four genes (ACCN1 to ACCN4) encode at least six different ASIC subunits (**Table 1**) sharing more than 50% amino acid identity: ASIC1a, ASIC1b, ASIC2a, ASIC2b, ASIC3, ASIC4 (ASIC5, also named BLINaC/BASIC and coded by the ACCN5 gene, only shares 30% amino acid identity and cannot be considered as a genuine ASIC subunit). The difference between the a and b variants of ASIC1 and ASIC2 relies on the first N-terminal third of the subunit (**Figure 1B**), including the cytoplasmic N-terminal domain, the re-entrant loop (forming part of the pore with the HG motif), the first transmembrane domain TM1 (forearm and wrist domains), and part of the extracellular loop (the palm  $\beta 1$  and  $\beta 3$  sheets, the  $\beta$ -ball  $\beta 2$  sheet and the entire finger domain).

**Table 1. Protein sequence comparison of rat and human ASIC subunits.**

Isoform	Species	% Identity	Size (aa)	Name in Genbank	Sequence ID
ASIC1a	<i>Rattus norvegicus</i>	98.11%	526	ASIC1	NP_077068.1
	<i>Homo sapiens</i>		528	ASIC1 isoform b	NP_001086.2

Isoform	Species	% Identity	Size (aa)	Name in Genbank	Sequence ID
ASIC1b	<i>Rattus norvegicus</i>	93.24%	559	ASIC1 isoform X5	XP_006257440.1
	<i>Homo sapiens</i>		562	ASIC1 isoform c	NP_001243759.1
ASIC2a	<i>Rattus norvegicus</i>	99.02%	512	ASIC2 isoform MDEG1	NP_001029186.1
	<i>Homo sapiens</i>		512	ASIC2 isoform MDEG1	NP_001085.2
ASIC2b	<i>Rattus norvegicus</i>	98.83%	563	ASIC2 isoform MDEG2	NP_037024.2
	<i>Homo sapiens</i>		563	ASIC2 isoform MDEG2	NP_899233.1
ASIC3	<i>Rattus norvegicus</i>	83.68%	533	ASIC3	NP_775158.1
	<i>Homo sapiens</i>		531	ASIC3 isoform a	NP_004760.1
ASIC4	<i>Rattus norvegicus</i>	97.22%	539	ASIC4	NP_071570.2
	<i>Homo sapiens</i>		539	ASIC4 isoform 1	NP_061144.4

Percentages of amino acid (aa) identity were calculated using BLAST.

The first crystal structure of an ASIC was solved in 2007 by the group of E. Gouaux from cASIC1 (chicken ASIC1), the chicken ortholog of rat ASIC1a (rASIC1a) [1]. Each subunit was represented as a hand holding a ball and divided into finger, thumb, palm, knuckle,  $\beta$ -ball, wrist, and forearm (transmembrane domains) domains (**Figure 1C**). An “acidic pocket” containing several pairs of acidic amino acids is present at the interface of each subunit and was proposed to be one of the pH sensors of the channel, whereas cations may access the ion channel by lateral fenestrations, then moving into a broad extracellular vestibule just above the inactivation gate and the selectivity filter (i.e., the structural element in the narrowest part of the pore that determines ionic selectivity) (**Figure 1D**) [1][4]. The most noticeable structural difference between human (h) ASIC1a (hASIC1a) and cASIC1 is a longer loop that extends down from the  $\alpha$ 4-helix to the tip of the thumb, due to two extra amino acids (D298 and L299) absent in all other ASIC isoforms [5].

The lowest amino acid identity is 52% between cASIC1 and rASIC3, while rat and human ASIC orthologs show amino acid identities between 83.68% (for ASIC3) and 99.02% (for ASIC2a) (**Table 1**). Interestingly, hASIC3, but not rASIC3, has three splice variants (a, b, c), resulting in differences in the C-terminal domain, hASIC3a mRNA being the main isoform expressed in human neuronal tissues, although hASIC3c was also significantly detected. A higher level of sequence variability for the same isoform is observed between hASIC3a and rASIC3 or mouse ASIC3 (mASIC3) orthologs. While experimentally determined structures are still lacking for ASIC2 and ASIC3, recent major advances in structure prediction using machine learning have allowed the generation of models for those ASICs, shedding a new light on potential structural variations underlying the functional differences between ASICs [6].

## 2. pH-Dependency

Homo- or heterotrimeric cloned ASICs were found to be voltage-insensitive but highly pH-sensitive upon heterologous expression in *Xenopus* oocytes or in mammalian cell lines. They are sodium selective, with additional low calcium permeability for ASIC1a and hASIC1b [7][8][9]. They are activated by a fast-extracellular acidosis from conditioning physiological pH to acidic test pH and inactivated by sustained extracellular acidosis. Interestingly, rat and human ASIC3 channels can be also activated at neutral (7.4) pH by lipids (arachidonic acid and lysophosphatidylcholine) [10][11] and hASIC3a channels have been shown to be sensitive to both acidic and alkaline pH [12].

The ASIC2b and ASIC4 subunits do not form functional proton-gated channels by themselves, but ASIC2b can associate with other ASIC subunits to confer new properties and regulations to heterotrimeric channels [2][13][14]. ASIC currents are generally transient even if the acidification is maintained, but a sustained phase is associated with expression of ASIC3 or with the presence of the ASIC2b subunit in heterotrimers (**Figure 2**). A sustained plateau phase is also associated with hASIC1b current, but not with rASIC1b [9]. Two types of sustained currents have been described for ASIC3: a window current at pH around 7.0 (**Figure 2**) resulting from the overlap of pH-dependent activation and desensitization curves, and a sustained current induced by more acidic test pHs. The TM1 domain modulates the pH-dependent activation, thus contributing to the window current near physiological pH and, combined with the N-terminal domain, the TM1 domain is also the key structural element generating the low pH-evoked sustained current [15].

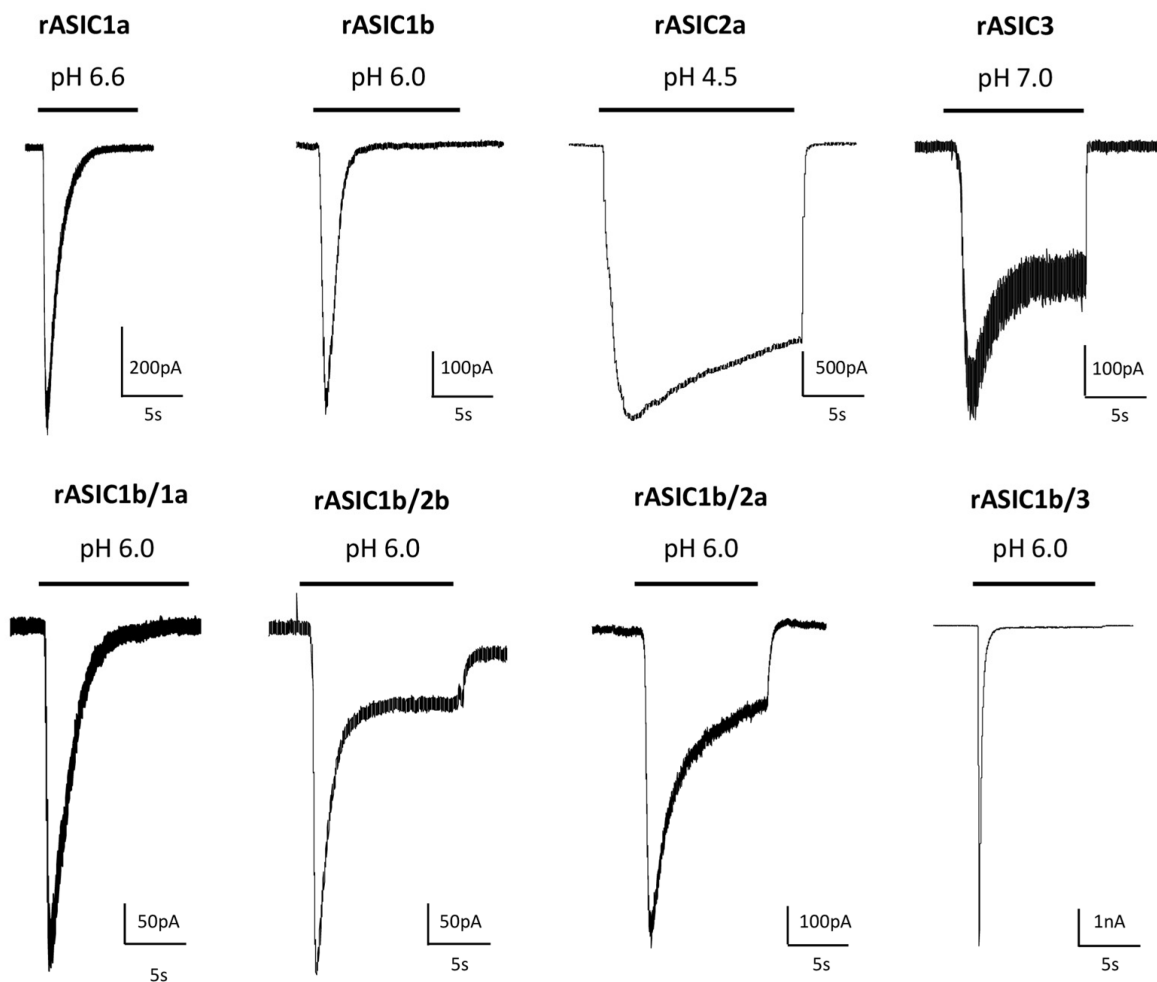


**Figure 2. Diversity of currents flowing through homo- and heterotrimeric cloned ASICs.** Original current traces of rat heterologously expressed ASIC currents recorded from HEK293 cells depending on the composition in ASIC subunits, activated from pH 7.4 to the indicated test pH, at  $-60$  mV. Homotrimeric channels result from the expression of only one type of ASIC subunit (indicated above each current), whereas heterotrimeric channels result from the co-expression of two different subunits (1:1 ratio in transfection). The corresponding current noted rASIC1b/1a, for example, results from the co-expression of rASIC1b and rASIC1a subunits.

ASICs differ in their biophysical properties depending on their subunit composition, notably in their desensitization time constants. rASIC3, rASIC1a and rASIC1b show significantly faster desensitization kinetics than rASIC2a (**Figure 2**). Experiments were conducted on heterologously expressed cloned channels by co-expressing two, or more rarely three (or concatemers), different subunits. The stoichiometry of association in heterotrimers (i.e., the relative number of each subunit in the channel) is therefore hard to precisely determine in these conditions. The ASIC1a and ASIC2a stoichiometry was at least investigated, showing no preferential association [16].

ASICs differ in their pH sensitivity, and the functional diversity obtained by combining the different subunits in homo- or heterotrimers (**Table 2**, with references in legend) allows these channels to detect a wide range of pH changes between pH 7.2 and pH 4.0. Sigmoidal curve fit of pH-dependent activation is used to determine the test  $pH_{0.5}$ , inducing the half-maximal activation that can vary between 6.8–6.3 (rASIC3) and 5.0–3.8 (rASIC2a). ASICs are desensitized depending on the conditioning pH, which is represented by the pH-dependent sigmoidal curve of steady-state desensitization (SSD) and by the conditioning  $pH_{0.5}$  of half-maximal SSD that can vary between 7.4–6.8 for rASIC1a and rASIC3 and 6.0–4.7 for hASIC2a (**Table 2**). These values are generally less acidic than the ones for activation, which means that the SSD mechanism in the presence of a sustained extracellular pH acidification will highly influence the amplitude of an ASIC current triggered by a subsequent rapid drop in pH. The sustained ASIC3 current results from incomplete inactivation and is activated at test pH 6.0 and below for hASIC3a and at pH 6.5 and below for rASIC3.

**Table 2. Functional pH ranges of currents flowing through cloned rodent and human ASICs.**



Cloned Channel	ACTIVATION		SSD	
	Test pH Threshold/max	pH <sub>0.5</sub>	Conditioning pH Threshold/max	pH <sub>0.5</sub>
rASIC1a	7.0/5.5	6.4–5.8 chimnqtwxyz	7.4/6.8	7.3–7.1 cehimtyz
rASIC1b	6.4/5.6	6.3–5.7 fitwxy#	7.3/6.6	7.0–6.5 fit#
m/rASIC2a	6.0/3.0	5.0–3.8 bnqwxz	7.0/4.5	6.3–5.6 mz
m/rASIC3	7.2/5.5	6.8–6.3 otwy	7.4/6.8	7.2–7.0 sty
rASIC1a/2a	6.3/4.5	5.6–4.8 nqrw		
m/rASIC1a/2b	6.8/6.0	6.4–6.2 pw	7.4/7.1	7.3 p
rASIC1a/1b		6.3–5.8 w		
rASIC1a/3	7.0/5.5	6.7–6.3 rtw	7.0/6.8	7.1 t
rASIC1b/3	6.6/5.9	6.7–6.2 tw	6.9/6.6	6.8 t
rASIC1b/2a		4.9 w		
rASIC2a/3	7.2/4.5	6.1–5.6 rw		
m/rASIC2a/2b		4.8 bw		
rASIC2b/3		6.5 w		
m/rASIC1a/2a/3		6.4–5.1 rw		
rASIC1a/2b/3		6.3 w		
rASIC1b/2a/3		4.9 w		
hASIC1a	6.8/6.0	6.6–6.3 dgikov	7.0/6.7	7.2–6.9 degiko
hASIC1b	6.5/5.5	5.9–5.7 gi	6.7/6.4	6.5–6.1 gi
hASIC2a	6.8/3.5	5.7 u	6.0/4.7	5.5 u
hASIC3a	7.0/5.5	6.6–6.2 aj	7.0/7.9	7.7–7.5 as
cASIC1	6.8/6.3	6.6 l	7.4/7.1	7.3 l

Representative pH ranges (threshold/max) and pH<sub>0.5</sub> values for pH-dependent activation of cellular ASIC currents activated from conditioning pH 7.4 to variable test pHs, and for pH-dependent steady state desensitization (SSD) of currents maximally activated from variable conditioning pHs with rat (r), mouse (m), chicken (c) and human (h) homotrimeric and heterotrimeric ASICs heterologously expressed in *Xenopus* oocytes or mammalian cell lines. The corresponding current noted rASIC1a/2a, for example, results from the co-expression of rASIC1a and rASIC2a subunits. References: a [17], b [18], c [19], d [20], e [21], f [22], g [9], h [23], i [24], j [12], k [25], l [26], m [27], n [28], o [29], p [30], q [31], r [32], s [33], t [34], u [35], v [36], w [3], x [37], y [38], z [39], # unpublished data.

### 3. pH-Dependent Gating

The molecular mechanism of pH-dependent gating of ASICs was studied through combined approaches including electrophysiology, mutagenesis, molecular dynamic simulations, X-ray crystallography and cryo-electron microscopy (cryo-EM), along with the pharmacological use of ASIC-targeting animal toxins.

The structures of the three conformational states involved in H<sup>+</sup>-dependent gating of homotrimeric cASIC1 were solved by X-ray crystallography and Cryo-EM: resting state [40] (**Figure 3A**), open state [41] (**Figure 3B**) and desensitized state [1] (**Figure 3C**). Cryo-EM structures of the hASIC1a in its closed state have also been solved, in complex with the snake toxin mambalgins-1 [42], and in complex with a specific nanobody Nb.C1 [5]. At the interface of each subunit of the trimeric channel, an acidic pocket is formed by intra-subunit contacts between the thumb, the β-ball and the finger domains, together with residues from the palm domain on the adjacent subunit (**Figure 1A,D** and **Figure 3**) [1][40].

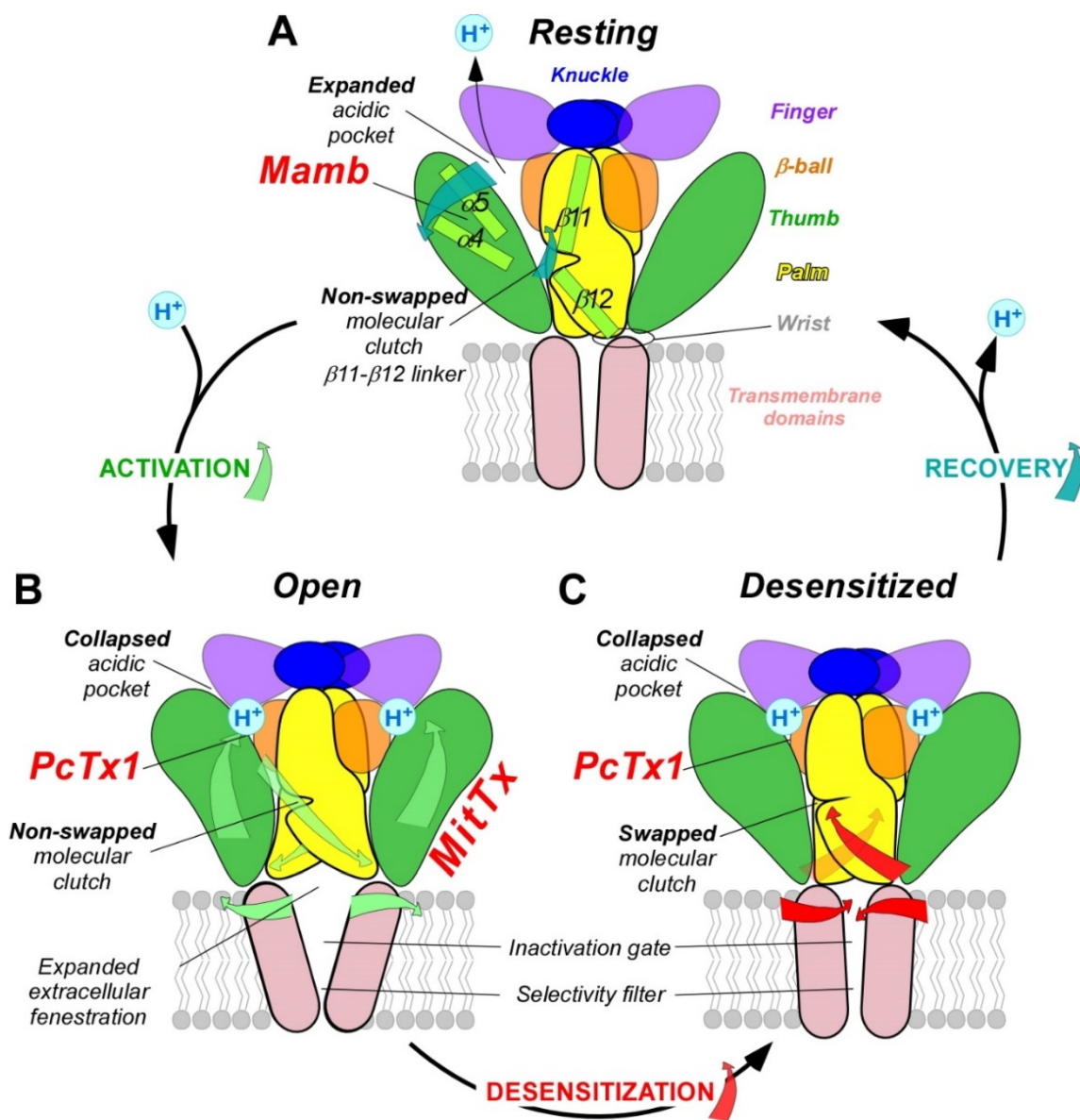


**Figure 3. pH-dependent gating mechanisms of ASICs and interaction with toxins.** ASIC gating involves three conformational states. (A), high pH resting state, which is stabilized by the snake toxin mambalgin (major domains involved are indicated with the same color code as in **Figure 1**). (B), low pH open state, which is stabilized by the snake toxin MitTx and also partially by the spider toxin PcTx1. (C), low pH desensitized state also promoted by PcTx1. To illustrate the recovery process in (A), the deprotonation mechanism of only one acidic pocket is presented. Blue (A), green (B) and red (C) arrows show critical conformational changes during recovery, activation and desensitization processes, respectively. For clarity, only two subunits are shown.

Upon activation by extracellular acidic pH, protonation of the acidic pocket (**Figure 3A,B**) leads to its collapsed conformation, which is stabilized by the formation of three pairs of carboxyl–carboxylate interactions between the side chains of aspartate and glutamate residues [41][40].  $\text{Cl}^-$  ion may play a role in channel gating by stabilizing the collapsed conformation of the acidic pocket at low pH, which seems state dependent since this bound  $\text{Cl}^-$  is absent in the resting state at high pH [43]. The motion of thumb helices  $\alpha$ 4/ $\alpha$ 5, resulting from collapse of the acidic pocket, induces a global motion of the thumb domain, which is directly connected to the transmembrane domain through a non-covalent contact forming a part of the wrist region [41][44]. In parallel, anchoring of the  $\alpha$ 5 helix against the palm of the adjacent subunit induces bending of the lower palm ( $\beta$ 1 and  $\beta$ 12 strands) toward the transmembrane domains (TM1 and TM2) to which they are covalently connected to form the other part of the wrist region. All together, thumb and lower palm domain motions lead to a rotation of each subunit around the scaffold formed by the knuckle and upper palm domains [40] that induces a translation of TM1 and TM2 leading to the expansion of extracellular fenestrations and to an iris-like opening of the channel gate (**Figure 3B**).

Ions are then enabled to pass through the selectivity filter of the pore (GAS belt motif, between TM2a and TM2b and HG motif in N-terminal re-entrant loop; **Figure 1C**) [41][44][45]. The Lys212 of the palm domain is deeply anchored to the thumb domain of the adjacent subunit and seems critical to facilitate the cooperativity between subunits during the global rotation of the extracellular domains of all the subunits [41][44][44][46]. In the lower palm domain, an inter-subunit hydrogen-bond

network, close to the wrist region, seems also critical for the correct propagation of conformational changes leading to the expansion of the extracellular fenestration [47][48] (**Figure 3B**). Several residues at the extracellular side of the transmembrane domain that form contacts within each subunit in desensitized and resting state [1][29] are disrupted after the iris-like opening of the pore [40]. It is interesting to note the arginine in this region that seems also necessary to mediate the potentiation of ASIC currents by lipids [49]. In addition to acid-induced activation, hASIC3 is also sensitive to alkalization, and this property is supported by two arginine residues only present in the human channel and also located close to the boundary between the plasma membrane and the extracellular medium [12].

During prolonged acidification, the  $\beta$ 11- $\beta$ 12 linker that demarcates the upper and lower palm domains undergoes a substantial conformational change induced by the switch in sidechain orientations of two residues [50][51][52]. This plays the role of “molecular clutch” allowing transmembrane domains to relax back into a “resting-like” conformation to permit rapid desensitization by uncoupling the conformational change of the upper extracellular domain from the lower part of the channel leading to the narrowing of the fenestration and the closing of the inactivation gate (**Figure 3C**) [40][51][52][53][54][55]. Just under the “molecular clutch”, a fourth pair of carboxyl–carboxylate interaction between the side chains of glutamate residues was identified [1] that probably influences its stability [56][57]. Moreover, the previously mentioned Lys212, in a loop immediately above the  $\beta$ 11- $\beta$ 12 linker, binds a  $\text{Cl}^-$  anion located in the thumb domain of an adjacent subunit [1][40][43] and could explain the mutations in the thumb domain also influencing desensitization [54][58][59][60].

Finally, when returning to physiological pH, the channel would return to the resting state after deprotonation of acidic residues that drive the expansion of the acidic pocket, allowing the  $\beta$ 11- $\beta$ 12 linker to revert back to a non-swapped conformation (**Figure 3A**) [40][51].

The intra- and inter-subunit network of H-bonds, salt bridges and carboxyl–carboxylate pairs involving several residues with different pKa values, highlights the complexity of the pH-dependent gating of ASICs and explains the different pH-dependent activation and desensitization characteristics of the various homo- or heterotrimeric channels in different species (**Table 2**), since several domains are directly or indirectly involved in both mechanisms via their intra- and inter-subunit connections.

Among the channels and receptors that respond to acidic pHs, only the proton-activated chloride channel (PAC) is, like ASICs, directly activated by protons through a complex and dedicated mechanism [61][62]. Interestingly, this channel also has a trimeric structure with a large extracellular domain, comprising fenestrations and acidic pockets, whose conformation change is transmitted to transmembrane domains after protonation. This suggests a complex convergent evolutionary process to achieve the pH sensing property of these two unrelated channels, albeit with completely different mechanisms at the molecular level. Very recently, a lysosomal proton (and  $\text{K}^+$ ) channel [63] with unrelated sequence and structure with ASICs was shown to be also activated by protons via a still unknown molecular mechanism. Proton-mediated gating of the capsaicin receptor TRPV1 is dependent of one key residue of the pore region (Phe660) [64], the inactivation of CNG channels is controlled by extracellular protons leading to the collapse of the pore via the titration of a single glutamate residue within the selectivity filter [65], and the two pore domain potassium channels ( $\text{K}_2\text{P}$ ) are modulated by protons through the titration of a key residue in the pore [66].

## **4. Pathophysiological Roles in Pain Sensing**

Relying on their pH-dependent gating properties, ASICs were involved in several functions associated with physiological and/or pathological extracellular pH variations [67][68][69][70][71][72][73][74][75]. We will focus here on pain sensing. Besides metabolic disorders producing systemic pH changes, there are other pathophysiological conditions that result in local pH variations, generally associated with increased pain perception. During pathophysiological conditions like inflammation, tissue injury, ischemia or cancer, extracellular pH can drop from physiological values (generally around 7.4) to values around 6.5 or even below. In rodent models, local extracellular pH can for instance decrease to 6.8–6.0 in implanted tumor, to 5.8 in carcinoma, to 6.0–4.0 in bone cancer, to 6.8 upon inflammation, to 5.7 in arthritis, to 6.5 in muscle after incision, to 6.9 during heart angina, to 6.9 in joints in osteoarthritis or rheumatoid arthritis, and to 6.5–6.2 in mouse brain after traumatic injury or stroke [76][77][78][79]. In humans, local extracellular pH was found to decrease to 6.0–5.4 in abscess, to 5.7–5.4 in human malignant tumors, to 7.0–6.0 in joint synovial fluid of osteoarthritis patients, to 6.9 in gout, to 6.4 in melanoma, or to 6.7 intracutaneously after muscle exercise [75][78], and localized skin tissue acidification ( $\text{pH} \geq 6.0$ ) causes pain in humans [80][81].

Tissue acidosis occurs therefore in a variety of pathological painful conditions, and ASIC subtypes expressed in nociceptive neurons have all the hallmarks of pain sensors. Several reviews have summarized the role of ASICs in the peripheral nervous system in nociception and also in proprioception [68][69][70][72][73][74][82]. ASICs are highly sensitive to

moderate acidifications, being for instance 10-fold more sensitive than the heat, capsaicin and proton-sensitive channel TRPV1 also expressed in peripheral sensory neurons. ASICs can generate sustained depolarizing currents upon prolonged tissue acidification compatible with the detection of non-adapting pain. Regulation of their activity by several pain-related mediators beside protons (inflammatory factors, neuropeptides, lipids, etc.) [11][83][84] led to the notion of coincidence detectors, especially for ASIC3, associated with pain detection and peripheral sensitization processes in pathophysiological situations like inflammation or chronic pain [75][85].

It is important to note that ASICs in the pain pathways are expressed not only in sensory neurons but also in dorsal horn neurons of the spinal cord involved in pain processing as well as in the brain, where they could be involved in synaptic transmission and plasticity, activated by the acidification of the synaptic cleft after the co-release of the acidic content of neurotransmitter synaptic vesicles, in particular in the case of chronic pain situations leading to central sensitization processes. Homotrimeric ASIC1a and heterotrimeric ASIC1a/2a were found to be postsynaptic receptors activated in several brain structures in glutamatergic and GABAergic neurons, where they could generate 3–10% of the synaptic current, even 20% at GABAergic synapses, and be involved in diverse forms of synaptic plasticity [74][86]. In the central nervous system, presynaptic or postsynaptic ASICs have thus been proposed to modulate learning and memory and to play a role in epilepsy and mood disorders as well as in neuronal damages associated with stroke and Alzheimer's disease [74][86][87].

---

## References

1. Jasti, J.; Furukawa, H.; Gonzales, E.B.; Gouaux, E. Structure of acid-sensing ion channel 1 at 1.9 Å resolution and low pH. *Nature* 2007, 449, 316–323.
2. Lingueglia, E.; de Weille, J.R.; Bassilana, F.; Heurteaux, C.; Sakai, H.; Waldmann, R.; Lazdunski, M. A modulatory subunit of acid sensing ion channels in brain and dorsal root ganglion cells. *J. Biol. Chem.* 1997, 272, 29778–29783.
3. Hesselager, M.; Timmermann, D.B.; Ahring, P.K. pH Dependency and Desensitization Kinetics of Heterologously Expressed Combinations of Acid-sensing Ion Channel Subunits. *J. Biol. Chem.* 2004, 279, 11006–11015.
4. Gonzales, E.B.; Kawate, T.; Gouaux, E. Pore architecture and ion sites in acid-sensing ion channels and P2X receptors. *Nature* 2009, 460, 599–604.
5. Wu, Y.; Chen, Z.; Sigworth, F.J.; Canessa, C.M. Structure and analysis of nanobody binding to the human ASIC1a ion channel. *eLife* 2021, 10, e67115.
6. Jumper, J.; Evans, R.; Pritzel, A.; Green, T.; Figurnov, M.; Ronneberger, O.; Tunyasuvunakool, K.; Bates, R.; Žídek, A.; Potapenko, A.; et al. Highly accurate protein structure prediction with AlphaFold. *Nature* 2021, 596, 583–589.
7. Waldmann, R.; Champigny, G.; Bassilana, F.; Heurteaux, C.; Lazdunski, M. A proton-gated cation channel involved in acid-sensing. *Nature* 1997, 386, 173–177.
8. Bassler, E.L.; Ngo-Anh, T.J.; Geisler, H.S.; Ruppersberg, J.P.; Grunder, S. Molecular and functional characterization of acid-sensing ion channel (ASIC) 1b. *J. Biol. Chem.* 2001, 276, 33782–33787.
9. Hoagland, E.N.; Sherwood, T.W.; Lee, K.G.; Walker, C.J.; Askwith, C.C. Identification of a Calcium Permeable Human Acid-sensing Ion Channel 1 Transcript Variant. *J. Biol. Chem.* 2010, 285, 41852–41862.
10. Jacquot, F.; Khoury, S.; Labrum, B.; Delanoe, K.; Pidoux, L.; Barbier, J.; Delay, L.; Bayle, A.; Aissouni, Y.; Barriere, D.A.; et al. Lysophosphatidylcholine 16: 0 mediates chronic joint pain associated to rheumatic diseases through acid-sensing ion channel 3. *Pain* 2022, 163, 1999–2013.
11. Marra, S.; Ferru-Clément, R.; Breuil, V.; Delaunay, A.; Christin, M.; Friend, V.; Sebillé, S.; Cognard, C.; Ferreira, T.; Roux, C.; et al. Non-acidic activation of pain-related Acid-Sensing Ion Channel 3 by lipids. *EMBO J.* 2016, 35, 414–428.
12. Delaunay, A.; Gasull, X.; Salinas, M.; Noël, J.; Friend, V.; Lingueglia, E.; Deval, E. Human ASIC3 channel dynamically adapts its activity to sense the extracellular pH in both acidic and alkaline directions. *Proc. Natl. Acad. Sci. USA* 2012, 109, 13124–13129.
13. Deval, E.; Salinas, M.; Baron, A.; Lingueglia, E.; Lazdunski, M. ASIC2b-dependent Regulation of ASIC3, an Essential Acid-sensing Ion Channel Subunit in Sensory Neurons via the Partner Protein PICK-1. *J. Biol. Chem.* 2004, 279, 19531–19539.
14. Sivils, A.; Yang, F.; Wang, J.Q.; Chu, X.-P. Acid-Sensing Ion Channel 2: Function and Modulation. *Membranes* 2022, 12, 113.

15. Salinas, M.; Lazdunski, M.; Lingueglia, E. Structural Elements for the Generation of Sustained Currents by the Acid Pain Sensor ASIC3. *J. Biol. Chem.* 2009, 284, 31851–31859.
16. Bartoi, T.; Augustinowski, K.; Polleichtner, G.; Gründer, S.; Ulbrich, M.H. Acid-sensing ion channel (ASIC) 1a/2a heteromers have a flexible 2:1/1:2 stoichiometry. *Proc. Natl. Acad. Sci. USA* 2014, 111, 8281–8286.
17. de Weille, J.R.; Bassilana, F.; Lazdunski, M.; Waldmann, R. Identification, functional expression and chromosomal localisation of a sustained human proton-gated cation channel. *FEBS Lett.* 1998, 433, 257–260.
18. Askwith, C.C.; Wemmie, J.A.; Price, M.P.; Rokhlina, T.; Welsh, M.J. Acid-sensing Ion Channel 2 (ASIC2) Modulates ASIC1 H<sup>+</sup>-activated Currents in Hippocampal Neurons. *J. Biol. Chem.* 2004, 279, 18296–18305.
19. Chen, X.; Kalbacher, H.; Grunder, S. The tarantula toxin psalmotoxin 1 inhibits acid-sensing ion channel (ASIC) 1a by increasing its apparent H<sup>+</sup> affinity. *J. Gen. Physiol.* 2005, 126, 71–79.
20. Sherwood, T.W.; Askwith, C.C. Endogenous Arginine-Phenylalanine-Amide-related Peptides Alter Steady-state Desensitization of ASIC1a. *J. Biol. Chem.* 2008, 283, 1818–1830.
21. Cristofori-Armstrong, B.; Saez, N.J.; Chassagnon, I.R.; King, G.F.; Rash, L.D. The modulation of acid-sensing ion channel 1 by PcTx1 is pH-, subtype- and species-dependent: Importance of interactions at the channel subunit interface and potential for engineering selective analogues. *Biochem. Pharmacol.* 2019, 163, 381–390.
22. Chen, X.; Kalbacher, H.; Grunder, S. Interaction of acid-sensing ion channel (ASIC) 1 with the tarantula toxin psalmotoxin 1 is state dependent. *J. Gen. Physiol.* 2006, 127, 267–276.
23. Diochot, S.; Baron, A.; Salinas, M.; Douguet, D.; Scarzello, S.; Dabert-Gay, A.-S.; Debayle, D.; Friend, V.; Alloui, A.; Lazdunski, M.; et al. Black mamba venom peptides target acid-sensing ion channels to abolish pain. *Nature* 2012, 490, 552–555.
24. Cristofori-Armstrong, B.; Budusan, E.; Rash, L.D. Mambalgins-3 potentiates human acid-sensing ion channel 1b under mild to moderate acidosis: Implications as an analgesic lead. *Proc. Natl. Acad. Sci. USA* 2021, 118, e2021581118.
25. Vaithia, A.; Vullo, S.; Peng, Z.; Alijevic, O.; Kellenberger, S. Accelerated Current Decay Kinetics of a Rare Human Acid-Sensing ion Channel 1a Variant That Is Used in Many Studies as Wild Type. *Front. Mol. Neurosci.* 2019, 12, 133.
26. Rook, M.L.; Miaro, M.; Couch, T.; Kneisley, D.L.; Musgaard, M.; MacLean, D.M. Mutation of a conserved glutamine residue does not abolish desensitization of acid-sensing ion channel 1. *J. Gen. Physiol.* 2021, 153, e202012855.
27. Baron, A.; Voilley, N.; Lazdunski, M.; Lingueglia, E. Acid sensing ion channels in dorsal spinal cord neurons. *J. Neurosci.* 2008, 28, 1498–1508.
28. Baron, A.; Schaefer, L.; Lingueglia, E.; Champigny, G.; Lazdunski, M. Zn<sup>2+</sup> and H<sup>+</sup> are coactivators of acid-sensing ion channels. *J. Biol. Chem.* 2001, 276, 35361–35367.
29. Chen, Z.; Kuenze, G.; Meiler, J.; Canessa, C.M. An arginine residue in the outer segment of hASIC1a TM1 affects both proton affinity and channel desensitization. *J. Gen. Physiol.* 2021, 153, e202012802.
30. Sherwood, T.W.; Lee, K.G.; Gormley, M.G.; Askwith, C.C. Heteromeric Acid-Sensing Ion Channels (ASICs) Composed of ASIC2b and ASIC1a Display Novel Channel Properties and Contribute to Acidosis-Induced Neuronal Death. *J. Neurosci.* 2011, 31, 9723–9734.
31. Bassilana, F.; Champigny, G.; Waldmann, R.; de Weille, J.R.; Heurteaux, C.; Lazdunski, M. The acid-sensitive ionic channel subunit ASIC and the mammalian degenerin MDEG form a heteromultimeric H<sup>+</sup>-gated Na<sup>+</sup> channel with novel properties. *J. Biol. Chem.* 1997, 272, 28819–28822.
32. Hattori, T.; Chen, J.; Harding, A.M.S.; Price, M.P.; Lu, Y.; Abboud, F.M.; Benson, C.J. ASIC2a and ASIC3 Heteromultimerize to Form pH-Sensitive Channels in Mouse Cardiac Dorsal Root Ganglia Neurons. *Circ. Res.* 2009, 105, 279–286.
33. Osmakov, D.I.; Koshelev, S.G.; Andreev, Y.A.; Kozlov, S.A. Endogenous Isoquinoline Alkaloids Agonists of Acid-Sensing Ion Channel Type 3. *Front. Mol. Neurosci.* 2017, 10, 282.
34. Chen, X.; Paukert, M.; Kadurin, I.; Pusch, M.; Gründer, S. Strong modulation by RFamide neuropeptides of the ASIC1b/3 heteromer in competition with extracellular calcium. *Neuropharmacology* 2006, 50, 964–974.
35. Malysz, J.; Scott, V.E.; Faltynek, C.; Gopalakrishnan, M. Characterization of human ASIC2a homomeric channels stably expressed in murine Ltk<sup>-</sup> cells. *Life Sci.* 2008, 82, 30–40.
36. Cho, J.-H.; Askwith, C.C. Potentiation of acid-sensing ion channels by sulfhydryl compounds. *Am. J. Physiol.-Cell. Physiol.* 2007, 292, C2161–C2174.
37. Salinas, M.; Rash, L.D.; Baron, A.; Lambeau, G.; Escoubas, P.; Lazdunski, M. The receptor site of the spider toxin PcTx1 on the proton-gated cation channel ASIC1a. *J. Physiol.* 2006, 570, 339–354.



38. Sutherland, S.P.; Benson, C.J.; Adelman, J.P.; McCleskey, E.W. Acid-sensing ion channel 3 matches the acid-gated current in cardiac ischemia-sensing neurons. *Proc. Natl. Acad. Sci. USA* 2001, 98, 711–716.
39. Salinas, M.; Besson, T.; Delettre, Q.; Diochot, S.; Boulakirba, S.; Douguet, D.; Lingueglia, E. Binding Site and Inhibitory Mechanism of the Mambalgin-2 Pain-relieving Peptide on Acid-sensing Ion Channel 1a. *J. Biol. Chem.* 2014, 289, 13363–13373.
40. Yoder, N.; Yoshioka, C.; Gouaux, E. Gating mechanisms of acid-sensing ion channels. *Nature* 2018, 555, 397–401.
41. Baconguis, I.; Bohlen, C.J.; Goehring, A.; Julius, D.; Gouaux, E. X-Ray Structure of Acid-Sensing Ion Channel 1–Snake Toxin Complex Reveals Open State of a Na<sup>+</sup>-Selective Channel. *Cell* 2014, 156, 717–729.
42. Sun, D.; Liu, S.; Li, S.; Zhang, M.; Yang, F.; Wen, M.; Shi, P.; Wang, T.; Pan, M.; Chang, S.; et al. Structural insights into human acid-sensing ion channel 1a inhibition by snake toxin mambalgin1. *eLife* 2020, 9, e57096.
43. Yoder, N.; Gouaux, E. Divalent cation and chloride ion sites of chicken acid sensing ion channel 1a elucidated by x-ray crystallography. *PLoS ONE* 2018, 13, e0202134.
44. Li, T.; Yang, Y.; Canessa, C.M. Interaction of the Aromatics Tyr-72/Trp-288 in the Interface of the Extracellular and Transmembrane Domains Is Essential for Proton Gating of Acid-sensing Ion Channels. *J. Biol. Chem.* 2009, 284, 4689–4694.
45. Yoder, N.; Gouaux, E. The His-Gly motif of acid-sensing ion channels resides in a reentrant 'loop' implicated in gating and ion selectivity. *eLife* 2020, 9, e56527.
46. Bargeton, B.; Kellenberger, S. The Contact Region between Three Domains of the Extracellular Loop of ASIC1a Is Critical for Channel Function. *J. Biol. Chem.* 2010, 285, 13816–13826.
47. Paukert, M.; Babini, E.; Pusch, M.; Gründer, S. Identification of the Ca<sup>2+</sup> Blocking Site of Acid-sensing Ion Channel (ASIC) 1. *J. Gen. Physiol.* 2004, 124, 383–394.
48. Paukert, M.; Chen, X.; Pollehn, G.; Schindelin, H.; Gründer, S. Candidate Amino Acids Involved in H<sup>+</sup> Gating of Acid-sensing Ion Channel 1a. *J. Biol. Chem.* 2008, 283, 572–581.
49. Klipp, R.C.; Bankston, J.R. Structural determinants of acid-sensing ion channel potentiation by single chain lipids. *J. Gen. Physiol.* 2022, 154, e202213156.
50. Baconguis, I.; Gouaux, E. Structural plasticity and dynamic selectivity of acid-sensing ion channel–spider toxin complexes. *Nature* 2012, 489, 400–405.
51. Wu, Y.; Chen, Z.; Canessa, C.M. A valve-like mechanism controls desensitization of functional mammalian isoforms of acid-sensing ion channels. *eLife* 2019, 8, e45851.
52. Li, T.; Yang, Y.; Canessa, C.M. Asn415 in the  $\beta$ 11– $\beta$ 12 Linker Decreases Proton-dependent Desensitization of ASIC1. *J. Biol. Chem.* 2010, 285, 31285–31291.
53. Rook, M.L.; Williamson, A.; Lueck, J.D.; Musgaard, M.; Maclean, D.M.  $\beta$ 11–12 linker isomerization governs acid-sensing ion channel desensitization and recovery. *eLife* 2020, 9, e51111.
54. Rook, M.L.; Ananchenko, A.; Musgaard, M.; MacLean, D.M. Molecular Investigation of Chicken Acid-Sensing Ion Channel 1  $\beta$ 11–12 Linker Isomerization and Channel Kinetics. *Front. Cell. Neurosci.* 2021, 15, 761813.
55. Rook, M.L.; Musgaard, M.; MacLean, D.M. Coupling structure with function in acid-sensing ion channels: Challenges in pursuit of proton sensors. *J. Physiol.* 2020, 599, 417–430.
56. Cushman, K.A.; Marsh-Haffner, J.; Adelman, J.P.; McCleskey, E.W. A Conformation Change in the Extracellular Domain that Accompanies Desensitization of Acid-sensing Ion Channel (ASIC) 3. *J. Gen. Physiol.* 2007, 129, 345–350.
57. Della Vecchia, M.C.; Rued, A.C.; Carattino, M.D. Gating Transitions in the Palm Domain of ASIC1a\*. *J. Biol. Chem.* 2013, 288, 5487–5495.
58. Krauson, A.J.; Carattino, M.D. The Thumb Domain Mediates Acid-sensing Ion Channel Desensitization. *J. Biol. Chem.* 2016, 291, 11407–11419.
59. Kusama, N.; Gautam, M.; Harding, A.M.S.; Snyder, P.M.; Benson, C.J. Acid-sensing ion channels (ASICs) are differentially modulated by anions dependent on their subunit composition. *Am. J. Physiol.-Cell. Physiol.* 2013, 304, C89–C101.
60. Kusama, N.; Harding, A.M.S.; Benson, C.J. Extracellular Chloride Modulates the Desensitization Kinetics of Acid-sensing Ion Channel 1a (ASIC1a). *J. Biol. Chem.* 2010, 285, 17425–17431.
61. Ruan, Z.; Osei-Owusu, J.; Du, J.; Qiu, Z.; Lu, W. Structures and pH-sensing mechanism of the proton-activated chloride channel. *Nature* 2020, 588, 350–354.

62. Osei-Owusu, J.; Kots, E.; Ruan, Z.; Mihaljevic, L.; Chen, K.H.; Tamhaney, A.; Ye, X.; Lu, W.; Weinstein, H.; Qiu, Z. Molecular determinants of pH sensing in the proton-activated chloride channel. *Proc. Natl. Acad. Sci. USA* 2022, 119, e2200727119.
63. Hu, M.; Li, P.; Wang, C.; Feng, X.; Geng, Q.; Chen, W.; Marthi, M.; Zhang, W.; Gao, C.; Reid, W.; et al. Parkinson's disease-risk protein TMEM175 is a proton-activated proton channel in lysosomes. *Cell* 2022, 185, 2292–2308.e2220.
64. Aneiros, E.; Cao, L.; Papakosta, M.; Stevens, E.B.; Phillips, S.; Grimm, C. The biophysical and molecular basis of TRPV1 proton gating. *EMBO J.* 2011, 30, 994–1002.
65. Marchesi, A.; Arcangeletti, M.; Mazzolini, M.; Torre, V. Proton transfer unlocks inactivation in cyclic nucleotide-gated A1 channels. *J. Physiol.* 2015, 593, 857–870.
66. Feliciangeli, S.; Chatelain, F.C.; Bichet, D.; Lesage, F. The family of K2P channels: Salient structural and functional properties. *J. Physiol.* 2015, 593, 2587–2603.
67. Kellenberger, S.; Schild, L.; Ohlstein, E.H. International Union of Basic and Clinical Pharmacology. XCI. Structure, Function, and Pharmacology of Acid-Sensing Ion Channels and the Epithelial Na<sup>+</sup> Channel. *Pharmacol. Rev.* 2015, 67, 1–35.
68. Karsan, N.; Gonzales, E.B.; Dussor, G. Targeted Acid-Sensing Ion Channel Therapies for Migraine. *Neurotherapeutics* 2018, 15, 402–414.
69. Lee, C.H.; Chen, C.C. Roles of ASICs in Nociception and Proprioception. *Adv. Exp. Med. Biol.* 2018, 1099, 37–47.
70. Deval, E.; Lingueglia, E. Acid-Sensing Ion Channels and nociception in the peripheral and central nervous systems. *Neuropharmacology* 2015, 94, 49–57.
71. Storozhuk, M.; Cherninskyi, A.; Maximyuk, O.; Isaev, D.; Krishtal, O. Acid-Sensing Ion Channels: Focus on Physiological and Some Pathological Roles in the Brain. *Curr. Neuropharmacol.* 2021, 19, 1570–1589.
72. Heusser, S.A.; Pless, S.A. Acid-sensing ion channels as potential therapeutic targets. *Trends Pharmacol. Sci.* 2021, 42, 1035–1050.
73. Lin, S.-H.; Sun, W.-H.; Chen, C.-C. Genetic exploration of the role of acid-sensing ion channels. *Neuropharmacology* 2015, 94, 99–118.
74. Lin, J.-H.; Hung, C.-H.; Han, D.-S.; Chen, S.-T.; Lee, C.-H.; Sun, W.-Z.; Chen, C.-C. Sensing acidosis: Nociception or sngception? *J. Biomed. Sci.* 2018, 25, 85.
75. Dulai, J.S.; Smith, E.S.J.; Rahman, T. Acid-sensing ion channel 3: An analgesic target. *Channels* 2021, 15, 94–127.
76. Ritzel, R.M.; He, J.; Li, Y.; Cao, T.; Khan, N.; Shim, B.; Sabirzhanov, B.; Aubrecht, T.; Stoica, B.A.; Faden, A.I.; et al. Proton extrusion during oxidative burst in microglia exacerbates pathological acidosis following traumatic brain injury. *Glia* 2020, 69, 746–764.
77. Lin, L.-H.; Jones, S.; Talman, W.T. Cellular Localization of Acid-Sensing Ion Channel 1 in Rat Nucleus Tractus Solitarii. *Cell. Mol. Neurobiol.* 2017, 38, 219–232.
78. Wood, J.N.; Stein, C.; Gaveriaux-Ruff, C. Opioids and Pain. In *The Oxford Handbook of the Neurobiology of Pain*; Oxford University Press: Oxford, UK, 2020; pp. 727–769.
79. Chesler, M. Regulation and Modulation of pH in the Brain. *Physiol. Rev.* 2003, 83, 1183–1221.
80. Ugawa, S.; Ueda, T.; Ishida, Y.; Nishigaki, M.; Shibata, Y.; Shimada, S. Amiloride-blockable acid-sensing ion channels are leading acid sensors expressed in human nociceptors. *J. Clin. Invest.* 2002, 110, 1185–1190.
81. Jones, N.G.; Slater, R.; Cadiou, H.; McNaughton, P.; McMahon, S.B. Acid-induced pain and its modulation in humans. *J. Neurosci.* 2004, 24, 10974–10979.
82. Ruan, N.; Tribble, J.; Peterson, A.M.; Jiang, Q.; Wang, J.Q.; Chu, X.-P. Acid-Sensing Ion Channels and Mechanosensation. *Int. J. Mol. Sci.* 2021, 22, 4810.
83. Wang, Y.; O'Bryant, Z.; Wang, H.; Huang, Y. Regulating Factors in Acid-Sensing Ion Channel 1a Function. *Neurochem. Res.* 2015, 41, 631–645.
84. Cullinan, M.M.; Klipp, R.C.; Bankston, J.R. Regulation of acid-sensing ion channels by protein binding partners. *Channels* 2021, 15, 635–647.
85. Deval, E.; Noël, J.; Lay, N.; Alloui, A.; Diochot, S.; Friend, V.; Jodar, M.; Lazdunski, M.; Lingueglia, E. ASIC3, a sensor of acidic and primary inflammatory pain. *EMBO J.* 2008, 27, 3047–3055.
86. Du, J.; Reznikov, L.R.; Price, M.P.; Zha, X.-m.; Lu, Y.; Moninger, T.O.; Wemmie, J.A.; Welsh, M.J. Protons are a neurotransmitter that regulates synaptic plasticity in the lateral amygdala. *Proc. Natl. Acad. Sci. USA* 2014, 111, 8961–8966.

87. Huang, Y.; Jiang, N.; Li, J.; Ji, Y.-H.; Xiong, Z.-G.; Zha, X.-m. Two aspects of ASIC function: Synaptic plasticity and neuronal injury. *Neuropharmacology* 2015, 94, 42–48.
- 

Retrieved from <https://encyclopedia.pub/entry/history/show/73363>